Available online www.jocpr.com

Journal of Chemical and Pharmaceutical Research, 2016, 8(6):184-205

Research Article

ISSN : 0975-7384
CODEN(USA) : JCPRC5

Vibrational spectra, nonlinear optical properties, NBO analysis and thermodynamic properties of N-phenylethanolamine by density functional method

V. Karunakaran[a] and V. Balachandran[b*]

[a]PG and Research Department of Physics, Government Arts College, Ariyalur 621 713, India
[b]Centre for Research , Department of Physics, A A Government Arts College, Musiri 621 211, India

---

ABSTRACT

In the present work, we reported a combined experimental and theoretical study on molecular structure and vibrational analysis of N-phenylethanolamine (NPEA). FT-IR and FT-Raman spectra of the title compound in the solid phase are recorded in the region 4000–400 cm^{-1} and 3500–100 cm^{-1}, respectively. The structural and spectroscopic data of the molecule in the ground state is calculated using density functional method with LSDA/6-311+G(d,p) and B3PW91/6-311+G(d,p) levels. The DFT (B3PW91/6-311+G(d,p)) calculations have been giving energies, optimized structures, harmonic vibrational frequencies, IR intensities and Raman activities. The study is extended to the HOMO–LUMO analysis to calculate the energy gap, ionization potential, electron affinity, global hardness, chemical potential and thermodynamic properties of NPEA. The calculated HOMO and LUMO energies show the charge transfer occurs in the molecule. A complete vibrational assignment aided by the theoretical harmonic frequency analysis has been proposed. The harmonic vibrational frequencies have been compared experimental FT-IR and FT-Raman spectra. The observed and calculated frequencies are found to be in good agreement. The complete vibrational assignments are performed on the basis of the total energy distribution (TED) of the vibrational modes calculated with scaled quantum mechanical (SQM) method.

Keywords: FT–IR spectra, FT–Raman spectra, N-phenylethanolamine, First order hyperpolarizability, Molecular electrostatic potential

---

INTRODUCTION

Phenylethanolamine is perhaps best known in the field of bioscience as part of the enzyme name “phenylethanolamine N-methyl transferase”, referring to an enzyme which is responsible for the conversion of norepinephrine into epinephrine, as well as other related transformations. In appearance, phenylethanolamine is a colorless solid [1].

Phenylethanolamine has been found to occur naturally in several animal species, including humans [2,3]. Phenylethanolamine (sometimes abbreviated PEOH), or β-hydroxyphenethylamine, is a biogenic amine related structurally to the major neurotransmitter norepinephrine, and the biogenic amine octopamine. As an organic compound, phenylethanolamine is a β-hydroxylated phenethylamine that is also structurally related to a number of synthetic drugs such as phenylpropanolamine, and the ephedrine family of alkaloids/drugs. In common with these compounds, phenylethanolamine has strong cardiovascular activity [4] and, under the name *Apophedrin*, has been used as a drug to produce topical vasoconstriction [5]. Chemically, phenylethanolamine is an aromatic compound, an amine, and an alcohol. The amino-group makes this compound a weak base, capable of reacting with acids to form salts. Phenylethanolamine was found to be an excellent substrate for the enzyme phenylethanolamine N-

methyl transferase (PNMT), first isolated from monkey adrenal glands by Julius Axelrod, which transformed it into N-methylphenylethanolamine [6].

EXPERIMENTAL SECTION

N-phenylethanolamine (NPEA) was procured by M/s Aldrich Chemicals, USA, which is of spectroscopic grade and hence used for recording the spectra as such without any further purification. The room temperature Fourier transform infrared spectrum of NPEA was measured in the region 4000–400 cm^{-1} at a resolution of ±1 cm^{-1} using a BRUKER IFS-66V FT-IR spectrometer equipped with a cooled MCT detector for the mid-IR range. KBr pellets were used in the spectral measurements. The FT-Raman spectra of NPEA were recorded on a BRUKER IFS-66V model interferometer equipped with an FRA-106 FT-Raman accessory in the region 3500–100 cm^{-1} using the 1064 nm line of a Nd:YAG laser for excitation operating at 200 mW power. The reported frequencies are expected to be accurate within ±1 cm^{-1}.

COMPUTATIONAL METHODS

The molecular structure of NPEA and corresponding vibrational harmonic frequencies were calculated using DFT/LSDA and B3PW91 combined with 6-311+G(d,p) basis set using Gaussian 09W program package [7] without any constraint on the geometry. The harmonic vibrational frequencies have been analytically calculated by taking the second-order derivative of energy using the same level of theory. Transformation of force field from Cartesian to symmetry coordinate, scaling, subsequent normal coordinate analysis, calculations of TED, IR and Raman intensities were made on a PC with the version V7.0–G77 of the MOLVIB program written by Sundius [8,9]. To achieve a close agreement between observed and calculated frequencies, the least-square fit refinement algorithm was used. By combining the results of the GAUSSVIEW [10] program with symmetry considerations, along with the available related molecules, vibrational frequency assignments were made with a high degree of accuracy.

Prediction of Raman intensities

The Raman intensities (I_i) were calculated from the Raman activities (S_i) obtained with the Gaussian 09W program, using the following relationship derived from the intensity theory of Raman scattering [11–13].

$$I_i = \frac{f(\upsilon_0 - \upsilon_i)^4 s_i}{\upsilon_i[1-\exp(-hc\upsilon_i)]/kT}$$

where υ_0 is the exciting frequency (in cm^{-1} units), υ_i is the vibrational frequency if the i^{th} normal mode, *h*, *c* and *k* are the universal constants and *f* is the suitably chosen common scaling factor for all the peak intensities. The simulated IR and Raman spectra have been plotted using Lorentzian band shapes with FWHM bandwidth of 10 cm^{-1}.

RESULTS AND DISCUSSION

Structural descriptions

In order to find the most optimized geometry, the energy calculations were carried out for N-phenylethanolamine, using LSDA/6-311+G(d,p) and B3PW91/6-311+G(d,p) methods for various possible conformers. The computationally predicted various possible conformers obtained for the title compound are shown in Fig.1. The total energies obtained for these conformers are listed in Table 1, the structure optimizations have shown that the conformer of Fig.1 (C6) have produced the global minimum energy. The optimized molecular structure with the numbering of atoms of the title compound is shown in Fig. 2. The most optimized structural parameters were also calculated by LSDA and B3PW91 levels and they are depicted in Table 2. The optimized structural parameters were used to compute the vibrational frequencies of the stable conformer (C6) of NPEA at the LSDA/6-311+G(d,p) and B3PW91/6-311+G(d,p) levels of calculations.

Table 1 Calculated energies of different conformations of N-phenylethanolamine molecule computed at LSDA/6-311+G(d,p) and B3PW91/6-311+G(d,p) levels

Conformers	LSDA/6-311+G(d,p)		B3PW91/6-311+G(d,p)	
	Energy(hartree)	Energy($kJmol^{-1}$)	Energy(hartree)	Energy($kJmol^{-1}$)
C1	–439.133666	–1152945.528594	–441.373507	–1158826.232630
C2	–439.129681	–1152935.066094	–441.362824	–1158798.182807
C3	–439.130556	–1152937.363751	–441.359624	–1158789.782092
C4	–439.132339	–1152942.043907	–441.369653	–1158816.112648
C5	–439.129691	–1152935.094011	–441.362833	–1158798.208550
*C6	–439.139355	–1152960.464459	–441.379603	–1158842.236312
C7	–439.125031	–1152922.857324	–441.358480	–1158786.778299
C8	–439.127371	–1152929.002475	–441.364403	–1158802.330410

**Global minimum energy*

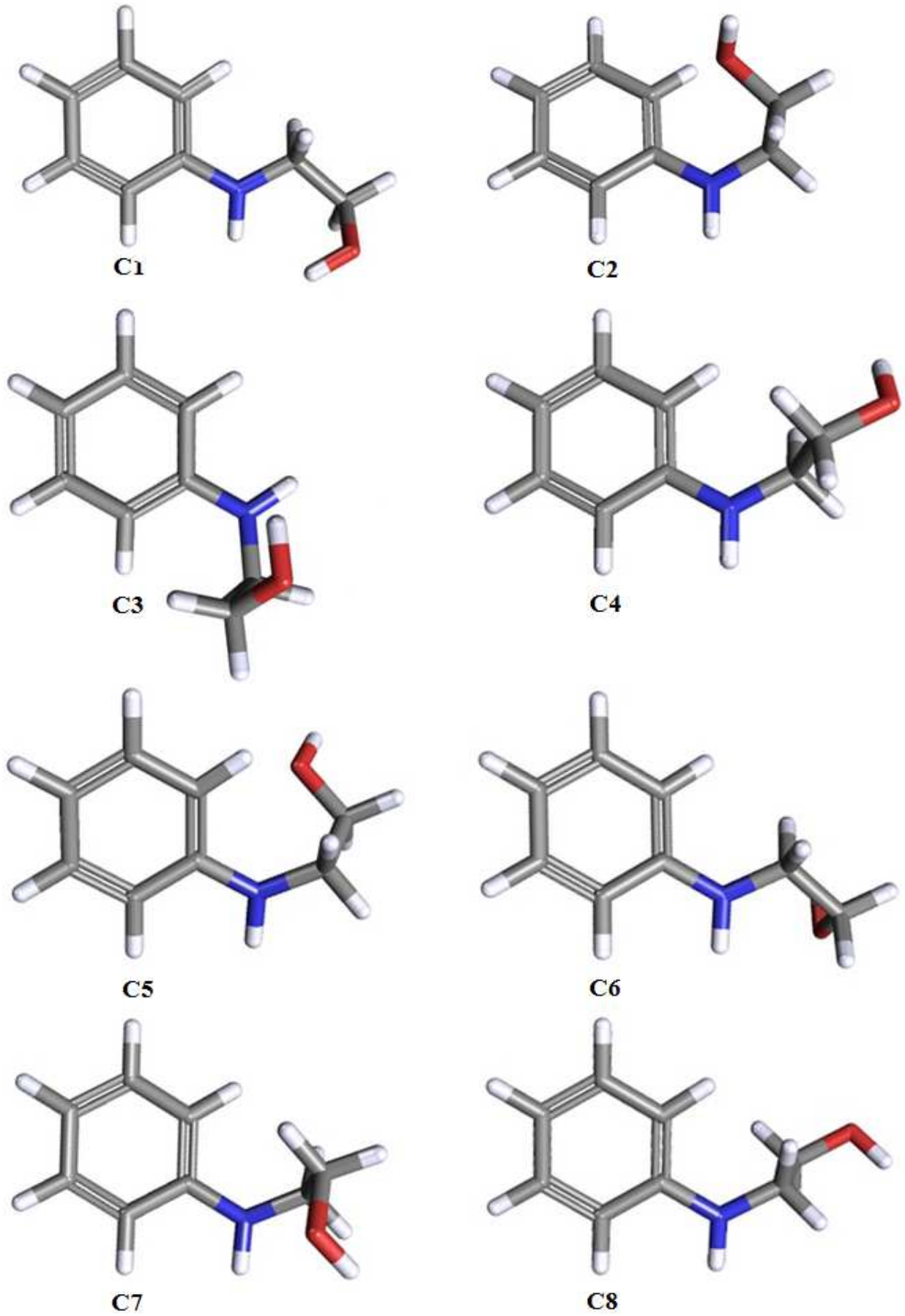

Fig. 1 Various possible conformers of N-phenylethanolamine

Vibrational assignments

In order to obtain the spectroscopic signature of the selected compound the harmonic-vibrational frequencies are calculated by DFT/LSDA and B3PW91 levels of theory with 6-311+G(d,p) basis set. The task of the vibrational analysis is to find out the different vibrational modes connected with specific molecular structure of title molecule. The molecular structure of NPEA belongs to C1 point group symmetry. The NPEA consists of 21 atoms; hence it undergoes 57 normal modes of vibrations.

Table 2 Optimized geometrical parameters for N-phenylethanolamine molecule computed at LSDA/6-311+G(d,p) and B3PW91/6-311+G(d,p) levels

Bond length(Å)	Value			Bond angle (°)	Value			Dihedral angle (°)	Value	
	LSDA	B3PW91	[a]Exp		LSDA	B3PW91	[a]Exp		LSDA	B3PW91
C_1-C_2	1.401	1.406		$C_2-C_1-C_6$	118.38	118.20		$C_6-C_1-C_2-C_3$	0.17	0.11
C_1-C_6	1.398	1.403		$C_2-C_1-N_7$	120.01	119.48		$C_6-C_1-C_2-H_{17}$	179.71	179.67
C_1-N_7	1.369	1.386		$C_6-C_1-N_7$	121.60	122.29		$N_7-C_1-C_2-C_3$	–178.73	–178.10
C_2-C_3	1.379	1.385		$C_1-C_2-C_3$	120.69	120.80		$N_7-C_1-C_2-H_{17}$	0.81	1.46
C_2-H_{17}	1.096	1.087		$C_1-C_2-H_{17}$	118.95	119.18		$C_2-C_1-C_6-C_5$	–0.39	–0.28
C_3-C_4	1.390	1.395		$C_3-C_2-H_{17}$	120.37	120.01		$C_2-C_1-C_6-H_{21}$	179.54	179.83
C_3-H_{18}	1.094	1.086		$C_2-C_3-C_4$	120.78	120.79		$N_7-C_1-C_6-C_5$	178.49	177.87
C_4-C_5	1.385	1.389		$C_2-C_3-H_{18}$	119.24	119.20		$N_7-C_1-C_6-H_{21}$	–1.57	–2.02
C_4-H_{19}	1.092	1.084		$C_4-C_3-H_{18}$	119.98	120.02		$C_2-C_1-N_7-H_8$	–21.18	–22.50
C_5-C_6	1.386	1.392		$C_3-C_4-C_5$	118.81	118.72		$C_2-C_1-N_7-C_9$	–168.82	–165.22
C_5-H_{20}	1.094	1.086		$C_3-C_4-H_{19}$	120.57	120.61		$C_6-C_1-N_7-H_8$	159.95	159.37
C_6-H_{21}	1.093	1.084		$C_5-C_4-H_{19}$	120.62	120.67		$C_6-C_1-N_7-C_9$	12.31	16.65
N_7-H_8	1.023	1.011		$C_4-C_5-C_6$	121.03	121.09		$C_1-C_2-C_3-C_4$	0.15	0.12
N_7-C_9	1.424	1.442		$C_4-C_5-H_{20}$	119.91	119.94		$C_1-C_2-C_3-H_{18}$	–179.99	–179.97
C_9-H_{10}	1.117	1.105		$C_6-C_5-N_{20}$	119.06	118.96		$H_{17}-C_2-C_3-C_4$	–179.38	–179.43
C_9-H_{11}	1.107	1.097		$C_1-C_6-C_5$	120.31	120.39		$H_{17}-C_2-C_3-H_{18}$	0.48	0.47
C_9-C_{12}	1.505	1.519		$C_1-C_6-H_{21}$	119.91	120.31		$C_2-C_3-C_4-C_5$	–0.26	–0.18
$C_{12}-H_{13}$	1.106	1.097		$C_5-C_6-H_{21}$	119.78	119.29		$C_2-C_3-C_4-H_{19}$	179.88	179.93
$C_{12}-H_{14}$	1.102	1.093		$C_1-N_7-H_8$	117.05	114.83		$H_{18}-C_3-C_4-C_5$	179.88	179.92
$C_{12}-O_{15}$	1.411	1.422		$C_1-N_7-C_9$	122.20	122.13		$H_{18}-C_3-C_4-H_{19}$	0.02	0.03
$O_{15}-H_{16}$	0.973	0.961		$H_8-N_7-C_9$	113.22	112.84		$C_3-C_4-C_5-C_6$	0.03	0.00
				$N_7-C_9-H_{10}$	111.91	112.00		$C_3-C_4-C_5-H_{20}$	–179.70	–179.80
				$N_7-C_9-H_{11}$	110.84	110.24		$H_{19}-C_4-C_5-C_6$	179.90	179.89
				$N_7-C_9-C_{12}$	108.72	109.81		$H_{19}-C_4-C_5-H_{20}$	0.16	0.09
				$H_{10}-C_9-H_{11}$	106.37	106.77		$C_4-C_5-C_6-C_1$	0.29	0.24
				$H_{10}-C_9-C_{12}$	109.96	109.76		$C_4-C_5-C_6-H_{21}$	–179.64	–179.88
				$H_{11}-C_9-C_{12}$	109.00	108.15		$H_{20}-C_5-C_6-C_1$	–179.97	–179.96
				$C_9-C_{12}-H_{13}$	110.19	109.60		$H_{20}-C_5-C_6-H_{21}$	0.09	–0.07
				$C_9-C_{12}-H_{14}$	109.54	109.77		$C_1-N_7-C_9-H_{10}$	56.29	54.02
				$C_9-C_{12}-O_{15}$	111.48	112.48		$C_1-N_7-C_9-H_{11}$	–62.28	–64.71
				$H_{13}-C_{12}-H_{14}$	108.01	108.06		$C_1-N_7-C_9-C_{12}$	177.94	176.23
				$H_{13}-C_{12}-O_{15}$	112.01	111.28		$H_8-N_7-C_9-H_{10}$	–92.47	–89.36
				$H_{14}-C_{12}-O_{15}$	105.43	105.48		$H_8-N_7-C_9-H_{11}$	148.97	151.91
				$C_{12}-O_{15}-H_{16}$	108.70	108.66		$H_8-N_7-C_9-C_{12}$	29.18	32.85
								$N_7-C_9-C_{12}-H_{13}$	–177.99	178.77
								$N_7-C_9-C_{12}-H_{14}$	63.32	60.23
								$N_7-C_9-C_{12}-O_{15}$	–52.97	–56.88
								$H_{10}-C_9-C_{12}-H_{13}$	–55.15	–57.70
								$H_{10}-C_9-C_{12}-H_{14}$	–173.84	–176.23
								$H_{10}-C_9-C_{12}-O_{15}$	69.87	66.66
								$H_{11}-C_9-C_{12}-H_{13}$	61.09	58.43
								$H_{11}-C_9-C_{12}-H_{14}$	–57.60	–60.10
								$H_{11}-C_9-C_{12}-O_{15}$	–173.89	–177.22
								$C_9-C_{12}-O_{15}-H_{16}$	–68.44	–69.12
								$H_{13}-C_{12}-O_{15}-H_{16}$	55.55	54.30
								$H_{14}-C_{12}-O_{15}-H_{16}$	172.78	171.25

Of the 57 normal modes of vibrations, 21 modes are stretching vibrations, 18 are in-plane bending modes of vibrations and remaining 18 modes are out-of-plane bending vibrations. The total energy distribution (TED) was calculated and the fundamental vibrational modes were characterized by their TED. The recorded (FT-IR, FT-Raman) and calculated vibrational wavenumber along with their relative intensities and probable assignments along with TED of the title molecule are given in Table 3. The experimental and theoretically predicted FT-IR and FT-Raman spectra are shown in Figs. 3 and 4, respectively.

To best of our knowledge, there is no theoretical study on the vibrational assignments of N-phenylethanolamine in the literature. So, in order to introduce detailed vibrational assignments of N-phenylethanolamine, a complete assignment of the fundamentals was proposed based on the calculated TED values, infrared and Raman intensities. Any inadequacy noted between the observed and the calculated frequencies may be due to the two facts: one is that the experimental results belong to solid phase and theoretical calculations belong to gaseous phase; the another one is that the calculations have been actually done on a single molecule contrary to the experimental values recorded in the presence of intermolecular interactions. The calculated vibrational frequencies were scaled in order to improve

the agreement with the experimental values. Vibrational frequencies calculated at LSDA/6-311+G(d,p) and B3PW91/6-311+G(d,p) levels were scaled by 0.9029 and 0.9623, respectively.

O–H vibrations

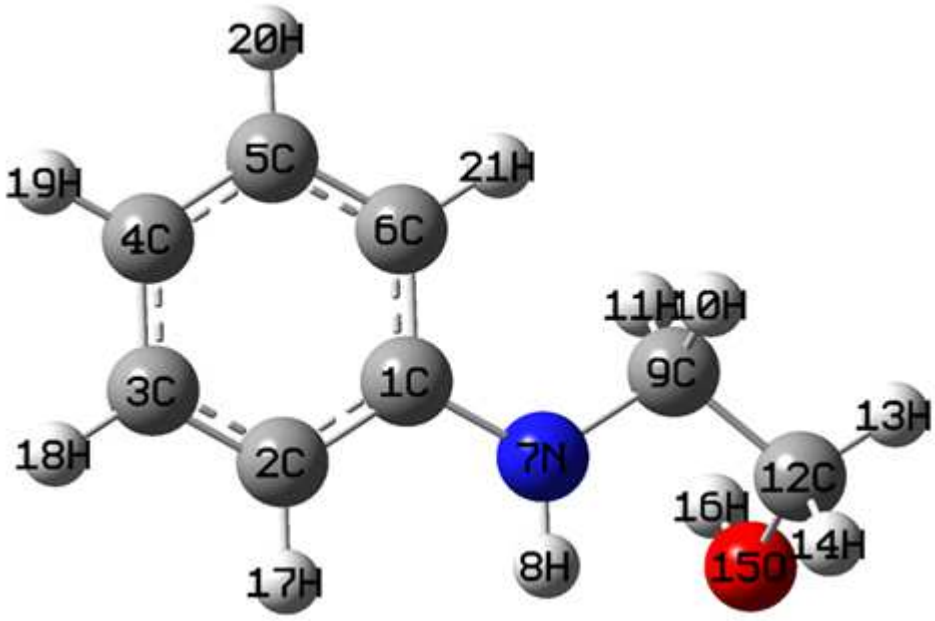

Fig. 2 The optimized molecular structure with numbering of atoms of N-phenylethanolamine

The O–H group gives rise to the three vibrations, viz. stretching, in-plane bending and out-of-plane bending vibrations. The O–H stretching vibrations are sensitive to hydrogen bonding [14]. The non-hydrogen-bonded hydroxyl group of phenols absorbs strongly in the 3700–3584 cm^{-1} region [15]. Hydrogen bonding alters the frequencies of the stretching and bending vibration. The O–H stretching bands move to lower frequencies usually with increased intensity and band broadening in the hydrogen bonded species.

Hydrogen bonding if present in five or six member ring system would reduce the O–H stretching band to 3550–3200 cm^{-1} region [16]. In the FT-IR spectrum of title compound, a medium strong band observed at 3323 cm^{-1} are assigned to O–H stretching mode of vibration. The TED contribution of this mode is 100%. A comparison of these bands with literature data predict that there is a deviation which may be due to the fact that the presence of intramolecular hydrogen bonding.

In general, for phenols the in-plane bending vibrations lay in the region 1250–1150 cm^{-1} [17]. In the present study, the O–H in-plane bending vibration calculated at 1288 cm^{-1} by LSDA/6-311+G(d,p) and 1286 cm^{-1} by B3PW91/6-311+G(d,p), respectively. They show good agreement with literature. The position of band due to O–H out-of-plane deformation vibration is dependent on the strength at hydrogen bond [18]. The O–H out-of-plane deformation vibration of phenol lies in the region 320–290 cm^{-1} for free O–H and in the region 710–571 cm^{-1} for associated O–H [17]. The frequency increase with hydrogen bond strength because of the larger amount of energy required to twist the O–H bond out-of-plane [19]. In our case the band observed in Raman spectrum at 285 cm^{-1} are assigned as O–H out-of-plane deformation vibration.

N–H vibrations

It has been observed that the presence of N–H in various molecules may be correlated with a constant occurrence of absorption bands whose positions are slightly altered from one compound to another; this is because of atomic group which vibrates independently from the other groups in the molecule and has its own frequency. In all the hetro cyclic compounds the N–H stretching vibrations occur in the region 3500–3300 cm^{-1} [20–22]. The position of absorption in this region depends upon the degree of hydrogen bonding and physical state of the sample. In the present investigation, the N–H stretching vibrations have been found at 3100 cm^{-1} in Raman spectrum with the 98% of TED contribution. Theoretically computed N–H vibrations by B3LYP method of scaled value approximately coincides with experimental value.

The bands observed at 1485 cm^{-1} and 743 cm^{-1} in Raman are assigned to N–H in-plane and out-of-plane bending vibrations, respectively.

Table 3 Vibrational assignments of fundamental observed frequencies and calculated frequencies of N-phenylethanolamine based on LSDA/6-311+G(d,p) and B3PW91/6-311+G(d,p) levels [Wavenumber (cm^{-1}); IR intensities (km mol^{-1}), Raman intensities ($Å^4amu^{-1}$) (Normalized to 100)]

Modes	Observed Frequencies (cm^{-1})		Calculated Frequencies (cm^{-1})				IR intensity		Raman intensity		Vibrational assignments/ TED(%)
			LSDA/6-311+G(d,p)		B3PW91/6-311+G(d,p)						
	FT-IR	FT-Raman	Unscaled	Scaled	Unscaled	Scaled	LSDA/6-311+G(d,p)	B3PW91/6-311+G(d,p)	LSDA/6-311+G(d,p)	B3PW91/6-311+G(d,p)	
1	3323ms		3725	3328	3855	3325	33.46	32.56	0.03	0.71	νOH(100)
2		3100ms	3469	3103	3601	3100	88.95	51.53	0.03	0.89	νNH(98)
3	2958w		3129	2958	3204	2956	5.02	6.17	0.04	1.04	νCHas(98)
4	2926ms	2927ms	3117	2930	3197	2928	11.72	26.02	0.04	0.46	νCHas(97)
5		2882w	3108	2885	3182	2880	7.89	20.07	0.04	1.48	νCHas(96)
6	2853w		3099	2850	3172	2851	3.18	1.90	0.04	1.61	νCHss(95)
7			3087	2845	3162	2840	7.78	10.61	0.04	0.67	νCHss(96)
8			3023	2836	3106	2832	15.24	23.19	0.04	1.16	CH_2as(95)
9			2953	2830	3042	2826	67.03	49.32	0.05	1.90	CH_2as(95)
10			2945	2825	3025	2819	6.22	39.37	0.05	2.05	CH_2ss(93)
11			2835	2816	2934	2810	88.48	78.47	0.05	2.50	CH_2ss(92)
12		1618vs	1647	1620	1662	1618	194.96	159.03	0.16	3.65	νCC(71), νCH(18), CH_2rock(10)
13	1603s		1609	1603	1636	1606	8.20	8.76	0.16	0.24	νCC(68), bCH(27)
14	1522s		1524	1525	1546	1520	241.07	201.33	0.18	0.16	νCC(70), νCH(15), CH_2sci(12)
15		1485s	1474	1489	1525	1486	6.05	0.67	0.19	0.37	bNH(52), bCC(33), bCH(10)
16	1456s	1456w	1437	1459	1503	1453	40.72	26.41	0.20	0.28	CH_2sci(68), bCH(24)
17	1397ms	1397ms	1426	1399	1493	1394	1.28	10.82	0.22	0.56	CH_2sci(68), bCH(23)
18	1382w		1420	1386	1467	1380	16.74	20.14	0.22	0.28	νCN(72), νCC(17)
19		1368w	1399	1373	1413	1369	36.54	27.02	0.23	0.24	CH_2wag(45), gOH(29)
20		1294ms	1352	1299	1384	1294	23.15	10.69	0.25	0.06	CH_2wag(46), gCH(30), gNH(11)
21			1330	1288	1377	1286	6.26	5.77	0.26	0.32	bOH(43), CH_2rock(25), bCH(13)
22	1279w		1322	1283	1369	1280	4.14	24.19	0.26	1.06	νCN(71), νCC(18)
23	1235ms	1234w	1298	1235	1349	1236	7.40	30.68	0.28	0.41	νCC(42), νCH(23), CH_2as(14)
24	1206ms	1206ms	1274	1210	1307	1203	9.41	66.80	0.29	0.77	νCC(43), bCH(22), CH_2rock(10)
25			1210	1196	1261	1192	20.25	5.91	0.30	0.47	νCC(42), νCH(20), bNH(18) CH_2rock(12)
26	1178w		1169	1162	1201	1178	6.59	19.48	0.32	0.20	νCO(47), νCH(22), CH_2ss(13)
27		1162ms	1154	1149	1200	1166	13.03	7.70	0.33	0.35	νCO(47), CH_2ss(),, CH_2rock(10)
28			1146	1124	1176	1120	28.74	1.85	0.34	0.43	CH_2twist(41), gCH(24), gCC(10)
29			1132	1103	1162	1098	0.98	21.22	0.35	0.39	CH_2twist(40), gCH(29), gCN(18)
30	1074s	1073w	1096	1078	1106	1074	57.23	5.17	0.37	0.11	bCH(58), νCO(21), bCN(14)
31	1044s	1044s	1076	1049	1096	1045	16.56	67.23	0.39	0.38	bCH(56), νCO(27), bNH(13)
32	1015w		1036	1020	1059	1016	7.70	38.71	0.41	0.10	bCH(55), νCO(28), bNH(11)
33		1002s	1017	1006	1054	1003	42.94	7.85	0.42	3.20	bCH(59), bOH(20), CH_2sci(12),
34		986vs	984	981	1004	988	2.08	3.86	0.44	4.67	bCH(58), νCO(18), bCC(10)
35	928w		944	935	983	930	0.18	0.11	0.48	0.04	gCH(45), gNH(13), gOH(10)
36		914ms	926	920	967	917	5.97	0.02	0.49	0.01	gCH(46), CH_2twist(14), gOH(10)
37	875vw		923	880	930	878	1.14	10.46	0.53	0.83	CH_2rock(39), bCH(22), bCN(15)

38		857ms	894	862	912	857	10.95	18.36	0.55	2.51	CH_2rock(40), bCH(20), bCC(13)
39		814w	845	819	879	816	6.31	4.60	0.60	0.09	bCN(43), bCH(30), bCC(14)
40		743s	809	747	828	745	2.16	1.43	0.69	1.12	gNH(51), gOH(24), CH_2twist(12)
41	717vs		784	721	818	717	1.15	1.80	0.73	0.50	bCN(42), bCH(28), bCC(10)
42	664w		739	668	761	665	43.78	60.36	0.82	0.36	gCH(44), gOH(31), gCN(17)
43		629w	681	631	701	630	49.14	35.78	0.90	0.04	gCH(45), gOH(30), CH_2wag(12)
44		601w	620	604	632	600	17.53	18.45	0.96	0.63	bCC(49), bCN(28), CH_2sci(11)
45		557w	614	556	629	555	0.48	0.05	1.09	1.05	gCH(43), gOH(32), gNH(18), CH_2wag(10)
46	523vw		570	527	567	523	130.3	134.68	1.19	1.10	bRing(50), bCH(27), bNH(16)
47	418vw		501	423	516	420	17.69	21.23	1.66	0.05	bRing(49), CH_2rock(18)
48		377w	472	378	472	375	8.78	9.35	1.98	0.70	gCN(44), gOH(22), CH_2twist(11)
49		354vw	416	359	417	355	21.09	10.80	2.15	1.11	bCO(41), bOH(28)
50		315vw	408	318	415	315	0.00	14.53	2.61	3.04	bRing(48), bCH(31), bCN(13)
51		285w	338	287	337	286	120.82	118.50	3.09	0.53	gOH(49), CH_2wag(28), gNH(10)
52			286	245	284	243	0.70	2.27	4.02	1.86	gCO(42), CH_2wag(30)
53		208ms	232	211	235	210	9.04	7.57	5.18	0.39	gCN(43), gNH(21), gOH(12)
54			186	155	182	152	1.05	0.94	8.81	1.26	gRing(42), CH_2twist(19)
55		116w	131	120	126	118	7.18	7.92	13.94	2.58	gRing(38), CH_2twist(16)
56			81	74	74	70	4.24	3.27	33.98	14.28	gCC(32), gRing(30), gOH(18)
57			54	42	55	43	0.80	0.43	100.00	100.00	gRing(36), Rtrigd(22), gOH(14)

s: strong; vs: very strong; ms: medium strong; w: weak; vw: very weak; ss: symmetric stretching; as: asymmetric stretching; b: in-plane bending; g: out-of-plane bending; v: stretching; sci: scissoring; rock: rocking; twist: twisting; wag: wagging.

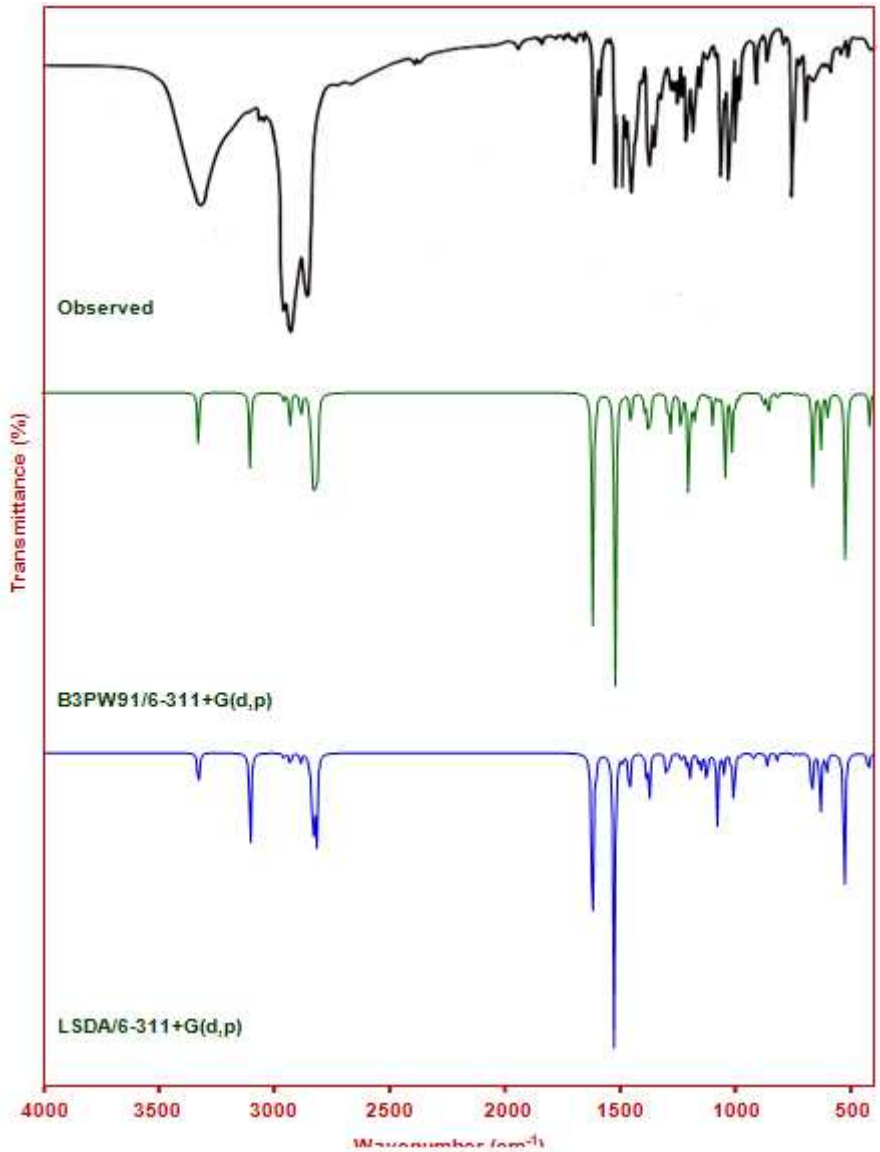

Fig. 3 The experimental and calculated FT-IR spectra of N-phenylethanolamine

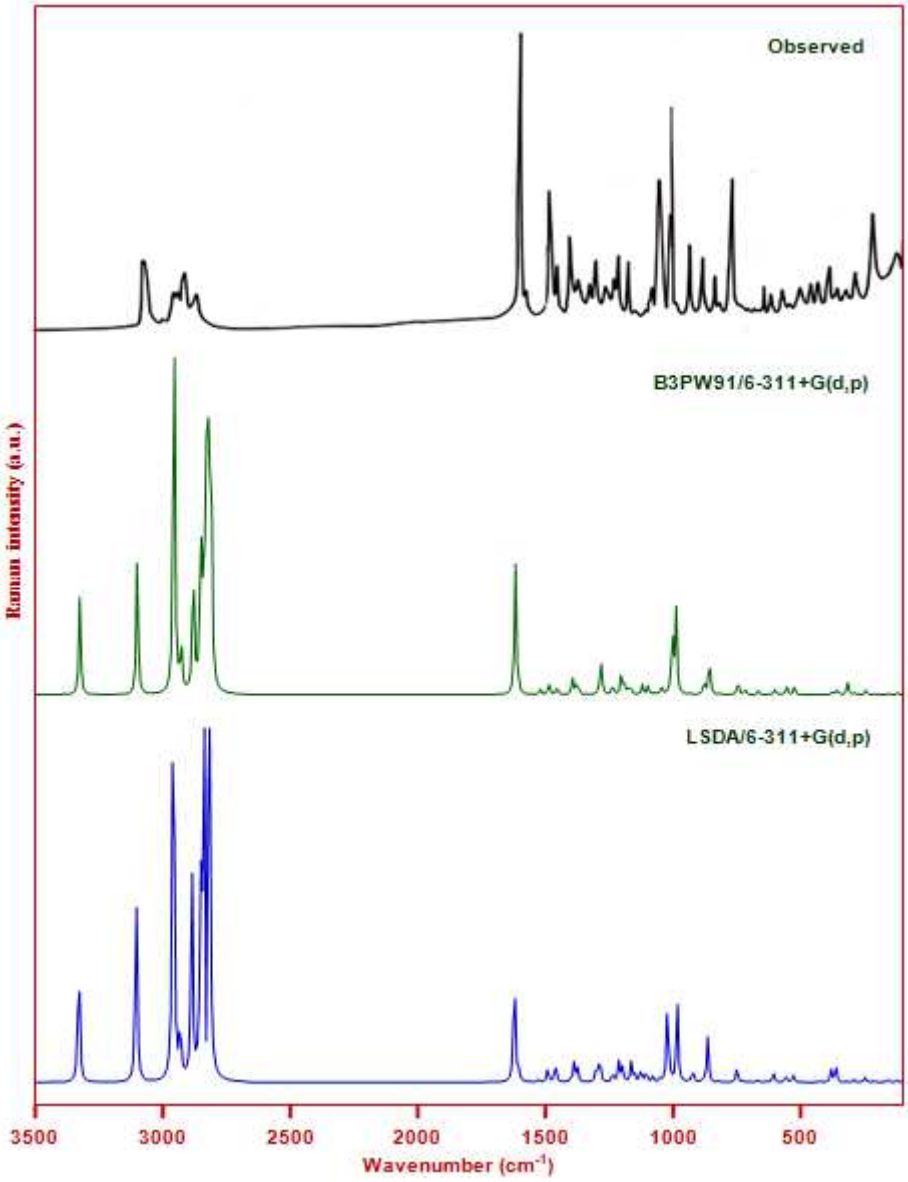

Fig. 4 The experimental and calculated FT-Raman spectra of N-phenylethanolamine

C–H vibrations

There are five C–H stretching vibrations in monosubstituted benzenes whose wavenumbers fall in the region 3120–3010 cm^{-1} [23]. The benzene derivatives are the best recognized among the polyatomic systems as far as the vibrational spectra are concerned [24,25]. The assignments of the benzene ring vibrations are relatively easy because these vibrations are observed at very similar wavenumbers in different compounds. The respective bands appear in the whole range of the spectrum [23].

In this region, the nature of the substituent does not make any appreciable change [26]. Gunasekaran *et al.* [27] have reported the presence of C–H stretching vibrations in the region 3100–3000 cm^{-1} for asymmetric stretching vibrations and 2990–2850 cm^{-1} for symmetric stretching vibrations. In this molecule, the FT-IR bands at 2958, 2926 cm^{-1} and FT-Raman bands at 2927, 2882 cm^{-1} have been assigned C–H asymmetric stretching vibrations. The FT-IR band at 2853 cm^{-1} represents C–H symmetric stretching vibration. The harmonic scaled frequencies by B3PW91/6-311+G(d,p) level predicted at 2956–2840 cm^{-1} fall within the recorded spectral range. As expected these modes are pure stretching modes as it is evident from TED column, they are exactly contributing to 95–98%.

The benzene ring C–H in-plane bending vibrations are usually weak and observed in the region 1300–1000 cm^{-1}, while the C–H out-of-plane bending vibrations lie in the region 900–650 cm^{-1} [24]. The C–H in-plane bending harmonic vibrations computed at 1074, 1045, 1016, 1003 and 988 cm^{-1} by B3PW91 method show excellent agreement with FT-IR bands at 1074, 1044 and 1015 cm^{-1} and FT-Raman bands at 1073, 1044, 1002 and 986 cm^{-1}

are assigned to C–H in-plane bending vibrations. The TED corresponds to this mode are mixed modes as it is evident from Table 3.

The C–H out-of-plane bending vibration of the title compound were well identified at 928 and 664 cm^{-1} in the FT-IR and 914, 629 and 557 cm^{-1} in the FT-Raman spectra are found to be well within their characteristic region and literature.

C–N vibrations

Because of the mixing of several bands, the identification of C–N vibrations is a very difficult task. Shanmugam *et al.* [28] assigned C–N stretching absorption in the region 1382–1266 cm^{-1}. In the present work, the bands observed at 1382 and 1279 cm^{-1} in FT-IR spectrum have been assigned to C–N stretching vibration. The computed values are in good agreement with recorded FT-IR spectrum of NPEA.

The FT-IR band at 717 cm^{-1} and the FT-Raman band at 814 cm^{-1} were assigned to C–N in-plane bending vibration. The C–N out-of-plane bending vibrations of the title compound were well identified at 354 and 208 cm^{-1} in the Raman spectrum. The TED of these modes suggests that this is a mixed mode.

C–O vibration

The absorption is sensitive for both the carbon and oxygen atoms of the carbonyl group. Both have the same while it vibrates. Normally, the C–O stretching vibrations occur in the region 1260–1000 cm^{-1} [29]. In the present study, the C–O stretching vibration observed in FT-Raman at 1162 cm^{-1} and computed at 1166 cm^{-1} for the title molecule at B3PW91/6-311+G(d,p) level. According to the literature, the C–O vibration is pushed to the lower region by the influence of other vibrations, because of the proximity. In NPEA, the C–O in-plane bending vibration is observed in FT-Raman at 354 cm^{-1} and found at 355 cm^{-1} at B3PW91/6-311+G(d,p) level, which is found mixed with the O–H in-plane bending mode.

The C–O out-of-plane bending vibration for the title molecule is assigned at 243 cm^{-1}. These assignments are agreement with the literature value [30].

CH_2 vibrations

The C–H stretching vibrations of the methylene group are at lower frequencies than those of the aromatic C–H stretching. The asymmetric CH_2 stretching vibration is generally observed in the region 3000–2900 cm^{-1}, while the CH_2 symmetric stretch will appear between 2900 and 2800 cm^{-1} [31,32]. The CH_2 asymmetric and symmetric stretching vibrations computed by the B3PW91/6-311+G(d,p) method at 2832, 2826, 2819 and 2810 cm^{-1} were assigned to CH_2 asymmetric and symmetric stretching modes of CH_2 unit. The TED corresponding to both (asymmetric and symmetric) type of vibrations show as pure modes of 92–97% as it is evident from the Table 3. The CH_2 bending modes follow, in decreasing wavenumber, the general order CH_2 deformation > CH_2 wagging > CH_2 twist > CH_2 rock. Since the bending modes involving hydrogen atom attached to the central carbon falls in the 1450–875 cm^{-1} range [33], there is extensive vibrational coupling of these modes with CH_2 deformations particularly with the CH_2 twist. It is notable that both CH_2 scissoring and CH_2 rocking modes were sensitive to the molecular conformation. For cyclohexane, the CH_2 scissoring mode has been assigned to the medium intensity IR band at about 1455 ± 55 cm^{-1} [32]. The CH_2 deformation band which comes near 1463 cm^{-1} in alkenes is lowered about 1440 cm^{-1} when the CH_2 group is next to a double or triple bond. A carbonyl, nitrile or nitro group lowers the wavenumber of the adjacent CH_2 group to about 1425 cm^{-1}. In our title molecule the scaled vibrational frequencies computed by B3PW91 method at 1453 and 1394 cm^{-1} are assigned to CH_2 scissoring modes of CH_2 unit showing good correlation with the recorded spectral data of strong bands at 1456, 1397 cm^{-1} in FT-IR spectrum and weak to medium bands at 1456, 1397 cm^{-1} in FT-Raman spectrum. The GaussView animation package suggests that it is a mixed mode with some contribution of bending vibration. The calculated TED corresponding to these modes are also as mixed mode with 68% of CH_2 scissoring mode.

The computed wavenumber by B3PW91 method at 1369 and 1294 cm^{-1} were assigned to CH_2 wagging vibrations for our title molecule which is in good agreement with the observed bands in FT-Raman at 1383 and 1294 cm^{-1}. The calculated TED corresponding to these modes are mixed modes with above 53% of CH_2 wagging. The bands for CH_2 rocking vibrations are observed at 875 cm^{-1} and 857 cm^{-1} respectively in FT-IR and FT-Raman spectra. The calculated frequencies of CH_2 rocking and CH_2 twisting vibrations are listed in Table 3. These are good agreement with the literature data.

C–C vibrations

The ring C–C stretching vibrations occur in the region 1625−1430 cm^{-1}. In general, the bands are of variable intensity and are observed at 1625–1590 cm^{-1}, 1590–1575 cm^{-1}, 1540−1470, 1465−1430 and 1380–1280 cm^{-1} as

given by Varasanyi [29] for the fine bands in this region. In the present work, the strong to weak bands observed in the FT-IR spectrum at 1603, 1522, 1235, 1206 and 1178 cm^{-1} have been assigned to C–C stretching vibrations in NPEA. The same vibrations appear in the FT-Raman spectrum at 1618, 1234 and 1206 cm^{-1}. The theoretically computed values by B3PW91/6-311+G(d,p) method at 1618, 1606, 1520, 1236, 1203 and 1178 cm^{-1} in NPEA showed excellent agreement with experimental data. The CCC in-plane bending vibrations observed at 523, 418 cm^{-1} in FT-IR spectrum and 601, 315 cm^{-1} in FT-Raman spectrum. The out-of-plane bending vibration appeared at 116 cm^{-1}. These assignments are in good agreement with the literature [34,35]. These observed frequencies show that, the substitutions in the ring to some extend affect the ring modes of vibrations. The theoretically computed value by B3PW91/6-311+G(d,p) method is in agreement with experimental values.

POLARIZABILITIES AND HYPERPOLARIZABILITIES

The development of organic NLO materials for device applications are required a multidisciplinary effort involving both theoretical and experimental studies in the fields of chemistry, physics, and engineering. Quantum-chemical calculations have made an important contribution to the understanding of the electronic polarization underlying the molecular NLO processes and the establishment of structure-property relationships [36,37]. The polarizabilities and hyperpolarizabilities characterize the response of a system in an applied electric field [38,39].

Electric polarizability is a fundamental characteristic of atomic and molecular systems [40]. Polarizabilities and hyperpolarizabilities could determine not only the strength of molecular interactions (such as the long-range intermolecular induction, and dispersion forces), the cross sections of different scattering and collision processes, but also the NLO of the system [41]. The theory of electric polarizability is a key element of the rational interpretation of a wide range of phenomena, from nonlinear optics [42] and electron scattering [43] to phenomena induced by intermolecular interactions [44].

$$E = E^0 - \mu_\alpha F_\alpha - \tfrac{1}{2}\alpha_{\alpha\beta}F_\alpha F_\beta - \tfrac{1}{6}\beta_{\alpha\beta\gamma}F_\alpha F_\beta F_\gamma + \ldots$$

where E^0 is the energy of the unperturbed molecules, F_α is the field at the origin and μ_α, $\alpha_{\alpha\beta}$ and $\beta_{\alpha\beta\gamma}$ are the components of dipole moment, polarizability and the first-order hyperpolarizabilities respectively. In this paper, we present values of the total static dipole moment (μ), the mean polarizability (α_o), the anisotropy of the polarizability ($\Delta\alpha$) and the mean first-order hyperpolarizability (β_0) as defined [45–49] in the following equation:

$$\mu = \sqrt{\left(\mu_x^2 + \mu_y^2 + \mu_z^2\right)}$$

$$\alpha_o = \frac{\alpha_{xx} + \alpha_{yy} + \alpha_{zz}}{3}$$

$$\Delta\alpha = \left[\frac{\left(\alpha_{xx} - \alpha_{yy}\right)^2 + \left(\alpha_{yy} - \alpha_{zz}\right)^2 + \left(\alpha_{zz} - \alpha_{xx}\right)^2}{2}\right]^{1/2}$$

The complete equation for calculating the magnitude of β from Gaussian 09W output is given a follows:

$$\beta_0 = \sqrt{\left(\beta_x^2 + \beta_y^2 + \beta_z^2\right)}$$

where,

$$\beta_x = \beta_{xxx} + \beta_{xyy} + \beta_{xzz}$$

$$\beta_y = \beta_{yyy} + \beta_{xxy} + \beta_{yzz}$$

$$\beta_z = \beta_{zzz} + \beta_{xxz} + \beta_{yyz}$$

The total static dipole moment, the mean polarizability, the anisotropy of the polarizability and the mean first-order hyperpolarizability of the title compound have been calculated using B3PW91/6-311+G(d,p) level. The conversion factor α, β and HOMO and LUMO energies in atomic and cgs units : 1 atomic unit (a.u.) = 0.1482×10^{-24} electrostatic unit (e.s.u.) for α; 1 a.u. = 8.6393×10^{-33} e.s.u. for β; 1 a.u. = 27.2116 eV (electron volt) for HOMO and LUMO energies.

Urea is one of the prototypical molecules used in the study of the NLO properties of molecular systems. It was used frequently as a threshold value for comparative purposes. The calculated values of α and β for the title compound are 16.0718×10^{-24} e.s.u. and 3.1921×10^{-30} e.s.u. as shown in Table 4. These are greater than those of urea (the α and β of urea are 3.7693 Å^3 and 0.37289 × 10^{-30} e.s.u. obtained by B3LYP/6-311++G(d,p) method [50]). Theoretically, the first hyperpolarizability of the title compound is of 5.3 times the magnitude of urea. Domination of particular components indicates a substantial delocalization of charges in that direction. The maximum β value may be due to π-electron cloud movement from donor to acceptor which makes the molecule highly polarized and the intra- molecular charge transfer possible. The presence of ICT is confirmed with the vibrational spectral analysis. From the magnitude of the first hyperpolarizability, the N-phenylethanolamine may be a potential applicant in the development of NLO materials.

Table 4 Electric dipole moment μ (debye), mean polarizability α_{tot} (×10^{-24} e.s.u.), anisotropy polarizability $\Delta\alpha$ (×10^{-24} e.s.u.) and first order hyperpolarizability β_{tot} (×10^{-30} e.s.u.) for N-phenylethanolamine based on B3PW91/6-311+G(d,p) level

Parameters	Values	Parameters	Values
μ_x	0.2997	β_{xxx}	44.0922
μ_y	0.7593	β_{xxy}	−61.0779
μ_z	0.3783	β_{xyy}	216.0040
μ	0.89967	β_{yyy}	−231.7888
α_{xx}	111.6063	β_{xxz}	−15.4409
α_{xy}	−12.9651	β_{xyz}	15.7194
α_{yy}	142.0219	β_{yyz}	53.4789
α_{xz}	−3.1104	β_{xzz}	57.8811
α_{yz}	−0.0624	β_{yzz}	1.7689
α_{zz}	71.7114	β_{zzz}	37.2466
α_{tot}	16.0718	β_{tot}	3.1921
$\Delta\alpha$	30.0441		

NATURAL BOND ORBITAL ANALYSIS

The NBO analysis is an efficient method to investigate the stereoelctronic interactions on the reactivity and dynamic behaviors of chemical compounds. NBO analysis [51] was originated as a technique for studying hybridization and covalency effects in polyatomic wave functions. The work of Foster and Weinhold was extended by Reed *et al.* [52] who employed NBO analysis that exhibited particularly H-bonded and other strongly bound Van der waals complexes. NBO calculations have been performed using NBO 3.1 program [53] as implemented in the Gaussian 09W program package [7] and GaussView molecular visualization program [10] at the B3PW91/6-311+G(d,p) level in order to understand various second-order interactions between the filled orbitals of one subsystem and vacant orbitals of another subsystem, which are a measure of the intermolecular delocalization or hyperconjugation.

A useful aspect of the NBO method is that it gives information about interactions in both filled and virtual orbital spaces, which could enhance the analysis of intra and intermolecular interactions. NBO method makes possible to examine hyperconjugative interactions due to electron transfers from filled bonding orbitals (donor) to empty anti-bonding orbitals (acceptor) [54–56]. In the compound examined hyperconjugative interactions are of second-order type and take place between σ and σ* orbitals or between electron lone-pairs (LPs) and σ* orbitals. The symbols σ and σ* are used in a generic sense to refer to filled and unfilled orbitals of the formal Lewis structure, though the former orbitals may actually be core orbitals (c), lone pairs (n), σ or π bonds (σ, π), etc., and the latter may be σ or π antibonds (σ*, π*), extra-valence-shell Rydberg (r) orbitals, etc., according to the specific case.

The second-order Fock matrix was used to evaluate the donor–acceptor interactions in the NBO basis [52]. The interactions result in a loss of occupancy from the localized NBO of the idealized Lewis structure into an empty non-Lewis orbital. For each donor (i) and acceptor (j), the stabilization energy $E^{(2)}$ associated with the delocalization i → j is estimated as [57]

$$E^{(2)} = \Delta E_{ij} = q_i \frac{F(i,j)^2}{\varepsilon_j - \varepsilon_i}$$

where q_i is the donor orbital occupancy, ε_i and ε_j are diagonal elements and F(i,j) is the off-diagonal NBO Fock matrix element. Hybrids of natural bond orbitals calculated by NBO analysis for the title compound are given in Table 5. The NBO bond polarization and hybridization changes were associated with formation of the compound. In NBO analysis, large $E^{(2)}$ value shows the intensive interaction between electron-donors and electron-acceptors and greater the extent of conjugation of the whole system, the possible intensive interactions are given in Table 6.

Table 5 NBO results showing of Lewis and non-Lewis orbitals of N-phenylethanolamine with B3PW91/6-311+G(d,p) level

Bond (A−B)	ED/energy (a.u.)	ED_A%	ED_B%	NBO	s%	p%
σ(C_1−C_2)	1.97500	50.81	49.19	0.7128($sp^{1.70}$) C	36.97	62.99
	0.02077			−0.7014($sp^{1.84}$) C	35.20	64.75
σ(C_1−C_6)	1.97401	50.60	49.40	0.7113($sp^{1.71}$) C	36.84	63.12
	0.02233			−0.7029($sp^{1.86}$) C	34.90	65.05
σ(C_1−N_7)	1.98783	39.25	60.75	0.6265($sp^{2.84}$) C	26.03	73.88
	0.02971			−0.7794($sp^{1.84}$) N	35.25	64.71
σ(C_2−C_3)	1.97604	50.52	49.48	0.7108($sp^{1.77}$) C	36.07	63.89
	0.01451			−0.7034($sp^{1.83}$) C	35.34	64.63
σ(C_2−H_{17})	1.97762	60.45	39.55	0.7775($sp^{2.48}$) C	28.70	71.27
	0.01385			−0.6289($sp^{0.00}$) H	99.96	0.04
σ(C_3−H_{18})	1.98007	60.43	39.57	0.7773($sp^{2.46}$) C	28.87	71.09
	0.01304			−0.6291($sp^{0.00}$) H	99.96	0.04
σ(N_7−C_9)	1.99025	60.96	39.04	0.7808($sp^{1.92}$) N	34.20	65.77
	0.01575			−0.6248($sp^{3.28}$) C	23.35	76.53
σ(C_{12}−O_{15})	1.99516	33.57	66.43	0.5794($sp^{3.65}$) C	21.47	78.33
	0.01418			−0.8150($sp^{2.37}$) O	29.64	70.28
σ(C_6−H_{11})	1.97730	60.67	39.33	0.7789($sp^{2.57}$) C	28.02	71.94
	0.01454			−0.6271($sp^{0.00}$) H	99.96	0.04
LP(1) N_7	1.80963	-	-	$sp^{1.00}$	0.00	100.00
LP(1) O_{15}	1.98262	-	-	$sp^{1.05}$	48.80	51.17
LP(2) O_{15}	1.96025	-	-	$sp^{99.99}$	0.08	99.88

Table 6 Second-order perturbation theory analysis of Fock matrix in NBO basic corresponding to the intra molecular bonds of N-phenylethanolamine with B3PW91/6-311+G(d,p) level

Donor (*i*)	Acceptor (*j*)	[a]$E^{(2)}$ (kJ mol^{-1})	[b]*E(j) – E(i)* (a.u.)	[c]*F(i,j)* (a.u.)
σ(C_1−C_2)	σ*(C_1−C_6)	3.94	1.28	0.064
σ(C_1−C_6)	σ*(C_1−C_2)	3.88	1.29	0.063
π(C_1−C_6)	π*(C_2−C_3)	17.34	0.29	0.063
	π*(C_4−C_5)	23.20	0.29	0.073
σ(C_2−C_3)	σ*(C_1−N_7)	4.47	1.06	0.062
π(C_2−C_3)	π*(C_1−C_6)	22.55	0.28	0.073
	π*(C_4−C_5)	17.35	0.28	0.064
σ(C_2−H_{17})	σ*(C_1−C_6)	4.63	1.10	0.064
π(C_4−C_5)	π*(C_1−C_6)	16.93	0.28	0.063
	π*(C_2−C_3)	22.56	0.28	0.071
σ(C_5−C_6)	σ*(C_1−N_7)	4.34	1.06	0.061
LP(1) N_7	π*(C_1−C_6)	30.24	0.27	0.086
	σ*(C_9−H_{10})	6.40	0.64	0.060
	σ*(C_9−H_{11})	6.25	0.65	0.059
LP(2) O_{15}	σ*(C_9−C_{12})	4.67	0.67	0.050
	σ*(C_{12}−H_{13})	6.12	0.71	0.059

[a]*$E^{(2)}$ means energy of hyperconjugative interactions.*
[b] *Energy difference between donor and acceptor i and j NBO orbitals.*
[c]*F(i,j) is the Fock matrix element between i and j NBO orbitals.*

In NBO analysis, the hyperconjugative σ → σ* interactions play a highly important role. These interactions represent the weak departures from a strictly localized natural Lewis structure that constitutes the primary "noncovalent" effects. The results of NBO analysis tabulated in Table 6 indicate that there are strong hyperconjugative interactions of σ(C2–C3) → σ*(C1–N7) [$E^{(2)}$ = 4.47 kJ mol^{-1}], σ(C2–H17) → σ*(C1–C6) [$E^{(2)}$ = 4.63 kJ mol^{-1}], σ(C5–C6) → σ*(C1–N7) [$E^{(2)}$ = 4.34 kJ mol^{-1}], LP(1) N7 → σ*(C9–H10) [$E^{(2)}$ = 6.40 kJ mol^{-1}] and LP(1) N7 → π*(C1–C6) [$E^{(2)}$ = 30.24 kJ mol^{-1}] for the title compound.

In interaction of σ(C2–C3) → σ*(C1–N7), C2 bond hybrid of the C2–C3 bond and C1 bond hybrid of the C1–N7 bond gains 26.03% in s character and 73.88% in p character (with hybrid orbital $sp^{2.84}$) by B3PW91 level (Table 5). These results show that strong intermolecular hyperconjugative interactions of the σ and π electrons between some part of the ethanolamine chain and the phenyl ring with different stabilization energies. On the other hand, the

intramolecular hyperconjugative interactions display π(C1–C6) → π*(C2–C3) [$E^{(2)}$ = 17.34 kJ mol^{-1}], π(C1–C6) → π*(C4–C5) [$E^{(2)}$ = 23.20 kJ mol^{-1}], π(C2–C3) → π*(C1–C6) [$E^{(2)}$ = 22.55 kJ mol^{-1}], π(C2–C3) → π*(C4–C5) [$E^{(2)}$ = 17.35 kJ mol^{-1}], π(C4–C5) → π*(C1–C6) [$E^{(2)}$ = 16.93 kJ mol^{-1}] and π(C4–C5) → π*(C2–C3) [$E^{(2)}$ = 22.56 kJ mol^{-1}] leading to stabilization of phenyl ring.

The most important interactions have occurred from the electron donating LP1 (N7) to the antibonding acceptor π*(C1–C6), σ*(C9–H10) and σ*(C9–H11) with stabilization energy from 30.24 to 6.25 kJ mol^{-1}. Likewise, LP2 (O15) conjugate with antibonding σ*(C12–H13) and σ*(C9–C12) leads to less stabilization energy of 6.12–4.67 kJ mol^{-1}. These interactions give rise to stabilization of phenyl ring. According to our results, the intramolecular charge transfer [n → π*, π → π*] occurs in title compound.

NATURAL HYBRID ORBITAL ANALYSIS

The natural hybrid orbitals (NHOs) result from a symmetrically orthogonalized hybrid orbital, which is derived from the natural atomic orbital (NAO) centered on particular atom through a unitary transformation [58]. According to the simple bond orbital picture, a NBO is defined as an orbital formed from NHOs. Therefore, for a localized σ-bond between atoms A and B, the NBO is defined as:

$$\sigma_{AB} = c_A h_A + c_B h_B$$

where h_A and h_B are the natural hybrids centered on atoms A and B and c_A and c_B are the polarization coefficients for atoms A and B.

The direction of each hybrid is specified in terms of the spherical polar angles theta (θ) and phi (φ) from the nucleus as well as the deviation angle *Dev* from the line of the centers between the bonded nuclei. For more general $sp^{\lambda}d^{\mu}$ hybrids, the hybrid direction is determined numerically to correspond to the maximum angular amplitude and then compared with the direction of the line of centers between the two nuclei to determine the bending of the bond, expressed as the deviation angle (*Dev*, in degrees) between these two directions. The angular properties of the natural hybrid orbitals are very much influenced by the type of substituent that causes the conjugative effect of steric effect. In Table 7, the bending angles of different bonds are expressed as the angle of deviation from the direction of the line joining the nuclei centers. Carbon of σCH is more bent away from the line of C_9–H_{14} centers by 2.7° in hybrid 1 and the line of C_9–H_{12} centers by 2.0° in hybrid 2, as a result of lying in the strong charge transfer path, whereas the carbon NHO is approximately aligned with the C–H axis. Similarly, a little lower bending effect (1.1°) is also noticed at the C–C and C–H groups.

Table 7 The NHO data obtained at B3PW91/6-311+G(d,p) level of theory for N-phenylethanolamine, which include NHO directionality and bending angles (deviations from line of nuclear centers)

NBO	Line of centers		Hybrid 1			Hybrid 2		
	θ	Φ	θ	φ	Dev	Θ	φ	Dev
σC_1–C_2	91.2	231.8	91.3	232.9	1.1	-	-	-
σC_1–C_6	83.3	111.8	83.4	109.7	2.0	-	-	-
πC_1–C_6	83.3	111.8	7.1	313.2	90.0	172.8	133.0	90.0
πC_2–C_3	84.5	172.1	172.9	132.4	90.0	7.1	312.3	90.0
σC_4–C_5	88.8	51.8	-	-	-	91.3	233.1	1.3
πC_4–C_5	88.8	51.8	7.2	312.3	90.0	172.8	132.4	90.0
σC_5–C_6	95.5	352.1	95.6	350.6	1.5	-	-	-
σC_9–H_{10}	29.0	101.2	27.6	102.2	1.5	-	-	-
σC_9–H_{11}	138.2	110.3	138.5	112.0	1.1	-	-	-
σC_9–H_{12}	96.3	341.6	96.6	340.5	1.1	82.3	163.0	2.0
σC_9–H_{13}	88.8	51.8	88.1	50.7	1.4	-	-	-
σC_9–H_{14}	151.0	281.2	148.4	282.3	2.7	-	-	-
σC_{12}–O_{15}	41.8	290.3	39.9	289.6	1.9	137.0	109.3	1.4
LP(1) N_7		-	7.1	308.0	-	-	-	-
LP(1) O_{15}	-	-	93.8	287.7	-	-	-	-
LP(2) O_{15}	-	-	88.5	19.1	-	-	-	-

HOMO-LUMO ANALYSIS

The HOMO (highest occupied molecular orbital)–LUMO (lowest unoccupied molecular orbital) energy gap of N-phenylethanolamine has been calculated at the B3PW91/6-311+G(d,p). Many organic molecules containing π conjugated electrons are characterized hyperpolarizabilities and were analyzed by means of vibrational spectroscopy [59,60]. These orbitals determine the way the molecule interacts with other species. Fig. 5 shows the distributions and energy levels of the HOMO–2, HOMO–1, HOMO, LUMO, LUMO+1 and LUMO+2 orbitals computed at the B3PW91/6-311+G(d,p) level for the title compound. HOMO is mainly localized on the methylene group and slightly delocalized in carbon atoms. LUMO is mainly delocalized in carbon atoms of phenyl ring. HOMO–1 is delocalized over the carbon atoms of phenyl ring and LUMO+1 is localized on the phenyl ring and methylene

group. HOMO–2 is delocalized over the hydroxyl group and LUMO+2 is localized on the hydroxyl group and methylene group. The value of the energy separation between the HOMO and LUMO is 5.18894 eV. The lowering of the HOMO–LUMO band gap is essentially a consequence of the large stabilization of the LUMO due to the strong electron-acceptor ability of the electron-acceptor group. The higher the energy of HOMO, the easier it is for HOMO to donate electrons whereas it is easier for LUMO to accept electrons when the energy of LUMO is low. The calculated energy values are presented in Table 8 which reveals the chemical reactivity of title compound and proves the occurrence of eventual charge transfer within the molecule.

Table 8 Selected HOMO and LUMO energies, energy gap values (eV) and related molecular properties of N-phenylethanolamine based on B3PW91/6-311+G(d,p) level

Molecular properties	Energy (eV)	Energy gap (eV)	Ionisation potential (I)	Electron affinity (A)	Global hardness (η)	Electro negativity (χ)	Global softness (σ)	Chemical potential (μ)	Global Electrophilicity (ω)
E_{total}(Hartree)	−441.3796								
E_{HOMO}	−5.56064	−5.18894	0.20435	0.01366	0.09535	0.10901	10.48768	−0.10901	0.06229
E_{LUMO}	−0.37170								
E_{HOMO-1}	−6.99006	−6.89319	0.25688	0.00356	0.12666	0.13022	7.89515	−0.13022	0.12128
E_{LUMO+1}	−0.09687								
E_{HOMO-2}	−7.91525	−7.74109	0.29088	0.00640	0.14224	0.14864	7.03037	−0.14864	0.12001
E_{LUMO+2}	−0.17415								

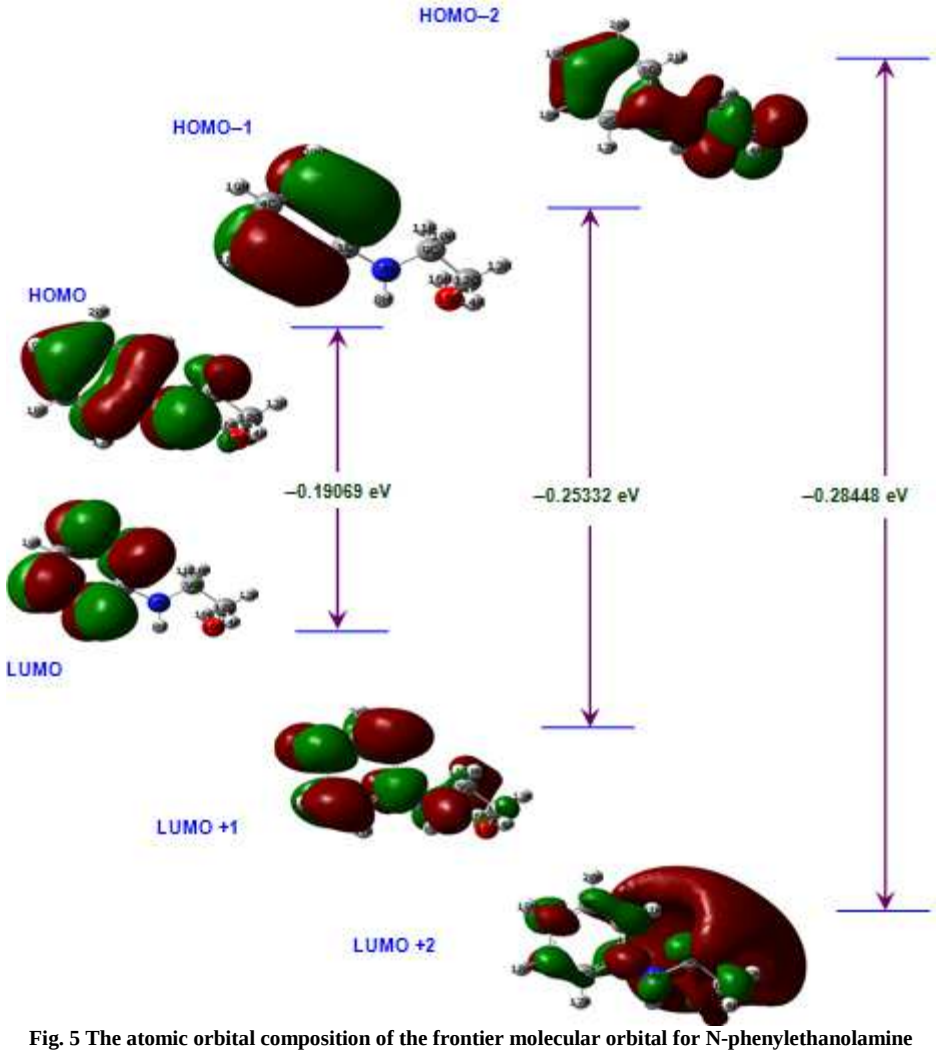

Fig. 5 The atomic orbital composition of the frontier molecular orbital for N-phenylethanolamine

Global and local reactivity descriptors

Based on the density functional descriptors, global chemical reactivity descriptors of title molecule such as global hardness (η), chemical potential (μ), global softness (σ),

electronegativity (χ), ionization potential (I), electron affinity (A) and global electrophilicity (ω) as well as local reactivity have been defined [61−64] as follows:

$$\eta = \frac{1}{2}\left(\frac{\partial^2 E}{\partial N^2}\right)_{V(r)} = \frac{1}{2}\left(\frac{\partial \mu}{\partial N}\right)_{V(r)}$$

$$\mu = \left(\frac{\partial E}{\partial N}\right)_{V(r)}$$

$$\chi = -\mu = -\left(\frac{\partial E}{\partial N}\right)_{V(r)}$$

where E is the total energy, N is the number of electrons of the chemical species, μ is the chemical potential and $V(r)$ is the external potential, which is identified as the negative of the electronegativity (χ) as defined by Iczkowski and Margrave [65]. According to Koopman's theorem [66], the entries of the HOMO and the LUMO orbital's of the molecule are related to the ionization potential (I) and the electron affinity (A), respectively, by the following reactions:

$$I = -E_{HOMO}$$

$$A = -E_{LUMO}$$

Absolute electronegativity (χ) and absolute hardness (η) of the molecule are given by [67], respectively. Softness (σ) is the reciprocal of hardness.

$$\chi = -\mu = \frac{1}{2}(I + A)$$

$$\eta = \frac{1}{2}(I - A)$$

$$\sigma = \frac{1}{\eta}$$

Recently Parr *et al*. [68] have defined a new descriptor to quantity of global electrophilic power of the compound as electrophilicity index (ω) in terms of chemical potential and hardness as follows:

$$\omega = \left(\frac{\mu^2}{2\eta}\right)$$

The usefulness of this new reactivity quantity understands the toxicity of various pollutants in terms of their reactivity and site selectivity. The calculated value of electrophilicity index describes the biological activity of NPEA. All the calculated values of quantum chemical parameters of the molecule using B3PW91/6-311+G(d,p) level are presented in Table 8.

Table 9 The electrostatic potential with atomic charge of N-phenylethanolamine based on B3PW91/6-311+G(d,p) level

Atom	Charge	Electrostatic potential (a.u.)
C1	0.497891	–14.728386
C2	–0.380812	–14.780884
C3	0.004287	–14.777364
C4	–0.112012	–14.787124
C5	–0.100173	–14.776910
C6	–0.311321	–14.781250
N7	–0.786918	–18.378244
H8	0.300168	–1.038723
C9	0.619450	–14.734759
H10	–0.105399	–1.110280
H11	–0.111713	–1.110549
C12	0.122163	–14.715539
H13	–0.026517	–1.110039
H14	0.030844	–1.104022
O15	–0.493016	–22.355360
H16	0.292727	–0.997371
H17	0.173774	–1.108759
H18	0.054719	–1.112936
H19	0.081903	–1.119554
H20	0.099601	–1.112462
H21	0.150354	–1.108065

ANALYSIS OF MOLECULAR ELECTROSTATIC POTENTIAL

Molecular electrostatic potential (MEP) at a point in the space around a molecule gives an indication of the net electrostatic effect produced at that point by the total charge distribution (electron + nuclei) of the molecule and correlates with dipole moments, electronegativity, partial charges and chemical reactivity of the molecules [33,69]. It provides a visual method to understand the relative polarity of the molecule. The different values of the electrostatic potential are represented by different colors; red represents the regions of the most negative electrostatic potential, white represents the regions of the most positive electrostatic potential and blue represents the region of zero potential. The potential increases in the order red < green < blue < pink < white. It can be seen that the negative regions are mainly over the O15 atom. The negative (red color) regions of MEP are related to electrophilic reactivity and the positive ones (white color) to nucleophilic reactivity. The negative electrostatic potential corresponds to an attraction of the proton by the aggregate electron density in the molecule (shades of red1), while the positive electrostatic potential corresponds to the repulsion of the proton by the atomic nuclei (shades of white). According to these calculated results, the MEP map shows that the negative potential sites are on oxygen and nitrogen atoms and the positive potential sites as well are around the aromatic hydrogen atoms. These sites give information concerning the region from where the compound can have metallic bonding and intermolecular interactions. The predominance of light green region in the MEP surfaces corresponds to a potential halfway between the two extremes red and dark blue color. The total electron density and MEP surfaces of the molecule under investigation are constructed by using B3PW91/6-311+G(d,p) method. The MEP mapped surface of the compound and electrostatic potential contour map for positive and negative potentials are shown in Figs. 6 and 7. The MEP map shows that the negative potential sites are on electronegative atoms, as well as the positive potential sites are around the hydrogen atoms. These sites give information about the region from where the compound can have non covalent interactions.

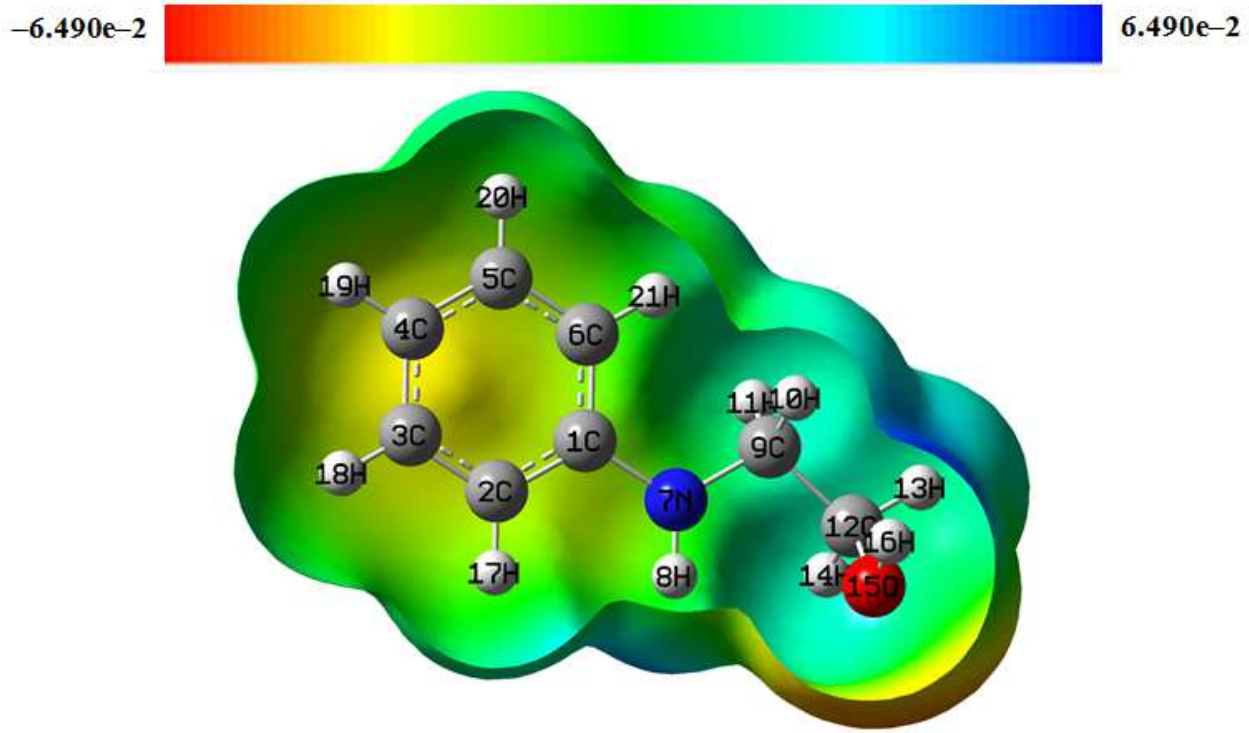

Fig. 6 The molecular electrostatic potential (MEP) of N-phenylethanolamine

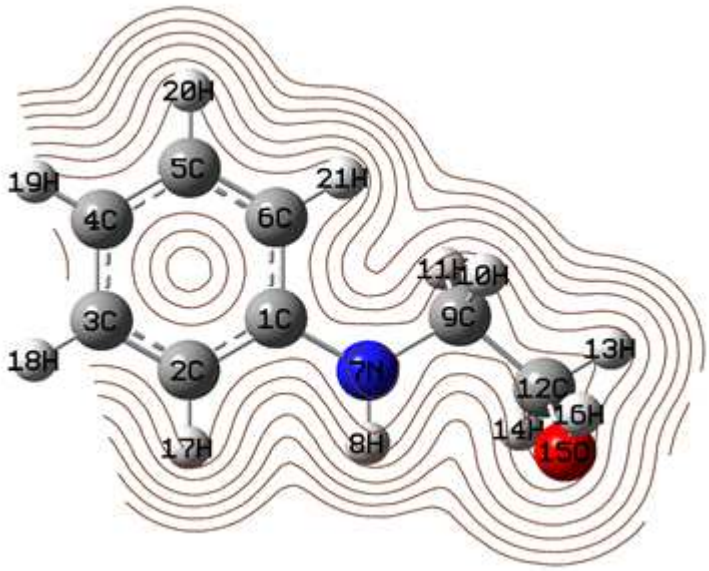

Fig. 7 The contour map of electrostatic potential of the total density of N-phenylethanolamine

MULLIKEN POPULATION ANALYSIS

The Mulliken atomic charges are calculated by determining the electron population of each atom as defined by the basis function [70]. The Mulliken atomic charges of NPEA molecule calculated by LSDA and B3PW91 levels with 6-311+G(d,p) basis set.

The calculation of effective atomic charges plays an important role in the application of quantum chemical calculations to molecular systems. Our interest here is in the comparison of different methods to describe the electron distribution in NPEA as broadly as possible, and assess the sensitivity, the calculated charges to changes in (i) the choice of the basis set; (ii) the choice of the quantum mechanical method. Mulliken charges, calculated the electron population of each atom defined in the basic functions. The Mulliken charges calculated at two different levels and at same basis set are listed in Table 10. The results can, however, better represent in graphical form as given Fig. 8. The charges depending on basis set are changed due to polarizability. The C6 atom has more positive charge both LSDA/6-311+G(d,p) and B3PW91/6-311+G(d,p), whereas the H16 atom has more positive charge than the other hydrogen atoms. This is due to the presence of electronegative oxygen atom; the hydrogen atom attracts the positive charge from the oxygen atom. The C5, C12 and O15 atoms by B3PW91 level are more negative charges than the other atoms due to electron accepting substitutions at that position in NPEA. The result suggests that the atoms bonded to O atom and all H atoms are electron acceptor and the charge transfer takes place from O to H in NPEA.

Table 10 Atomic charges for optimized geometry of N-phenylethanolamine based on LSDA/6-311+G(d,p) and B3PW91/6-311+G(d,p) levels

Atom No.	Mulliken charges	
	LSDA /6-311+G(d,p)	B3PW91/6-311+G(d,p)
C1	−0.401682	−0.204873
C2	−0.243334	−0.251215
C3	−0.280413	−0.261926
C4	−0.065650	−0.114014
C5	−0.888275	−0.778104
C6	0.842608	0.734935
N7	0.022622	−0.035686
H8	0.248224	0.250432
C9	−0.320566	−0.216910
H10	0.199449	0.166228
H11	0.200301	0.166278
C12	−0.437546	−0.392104
H13	0.198390	0.163576
H14	0.215524	0.179914
O15	−0.288954	−0.304135
H16	0.258165	0.242814
H17	0.134344	0.115679
H18	0.155929	0.138498
H19	0.151916	0.134450
H20	0.155257	0.138221
H21	0.143692	0.127943

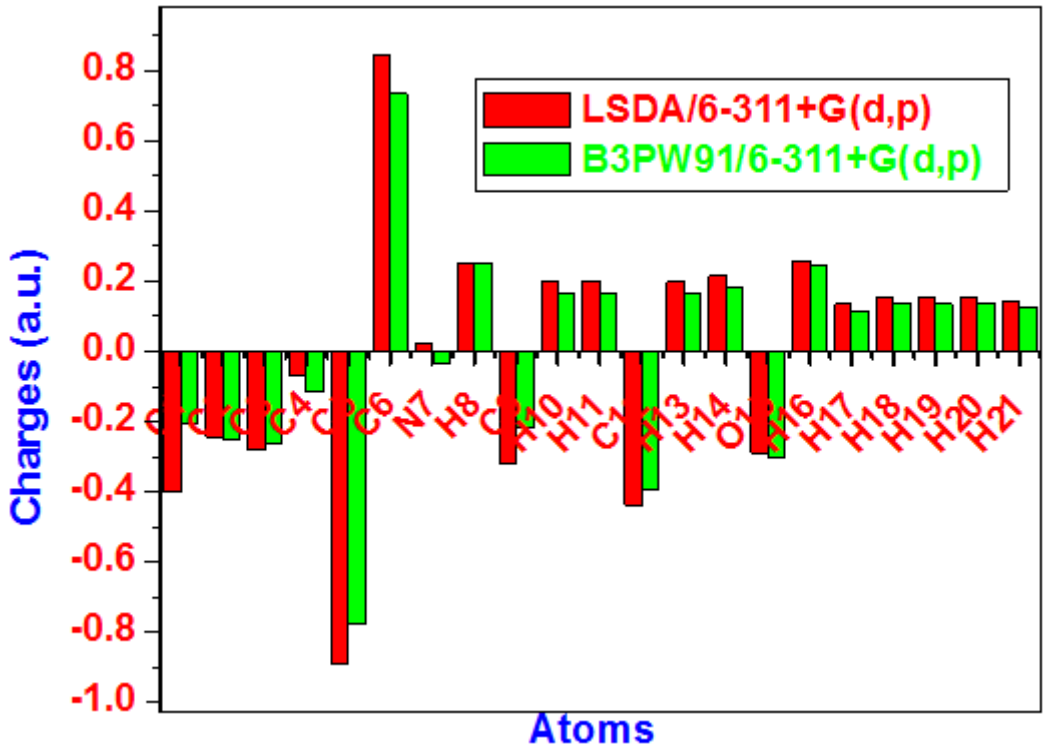

Fig. 8 Atomic charges correlation graph of N-phenylethanolamine

THERMODYNAMIC PROPERTIES

The total energy of a molecule is the sum of translational, rotational, vibrational and electronic energies. ie, E = Et + Er + Ev + Ee. The statistical thermochemical analysis of NPEA is carried out considering the molecule to be at room temperature of 298.15 K and one atmospheric pressure. The title molecule is considered as an asymmetric top having rotational symmetry number 1 and the total thermal energy has been arrived as the sum of electronic, translational, rotational and vibrational energies. The variations in the zero point vibrational energy seem to be insignificant.

The thermodynamic quantities such as heat capacity at constant pressure ($C^0_{p,m}$), enthalpy (ΔH^0_m), Gibb's free energy (G^0_m) and entropy (S^0_m) for various ranges (100K–1000K) of temperatures are determined and these results are presented in the Table 11. The correlation equations between these thermodynamic properties and temperatures were fitted by parabolic formula. The corresponding fitting equations are as follows and the correlation graphs are shown in Fig. 9.

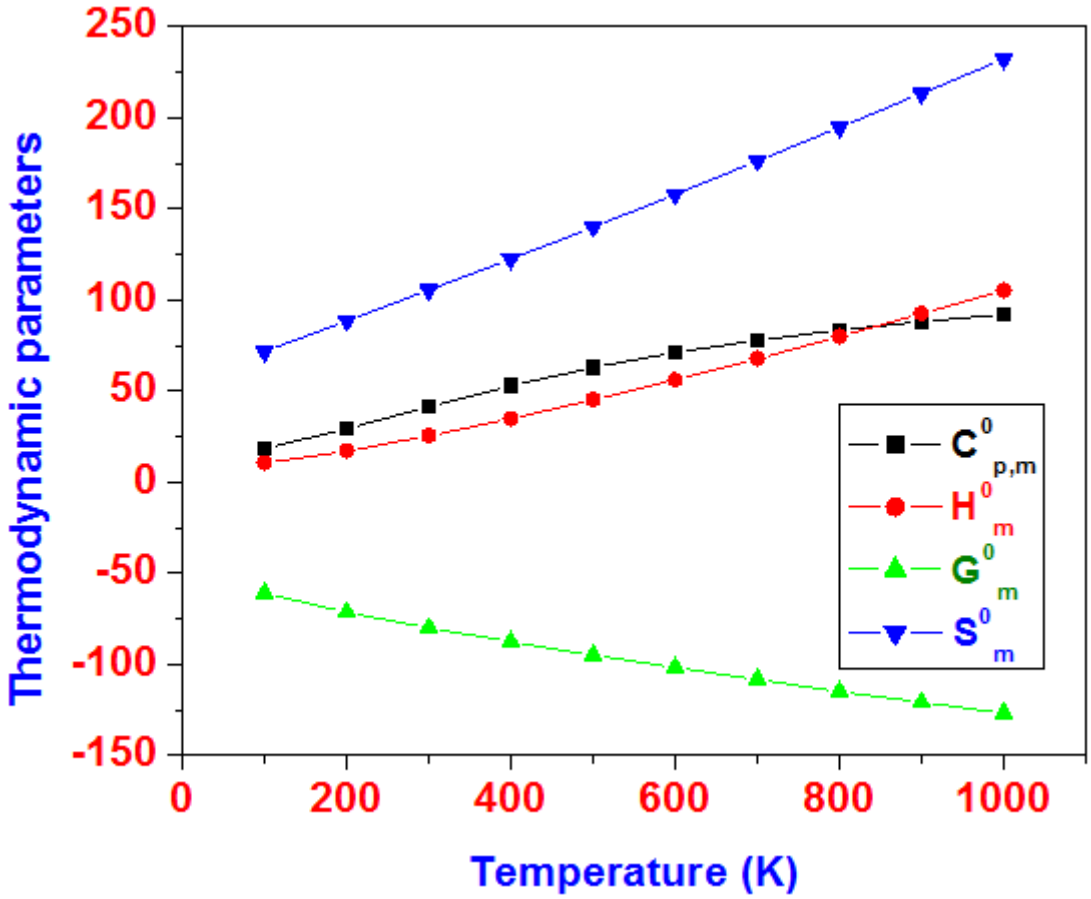

Fig. 9 Correlation graph of heat capacity, enthalphy, Gibb's energy and entropy with temperature of N-phenylethanolamine

All the thermodynamic data provide helpful information for the further study on the title compound. From the Table 11, it can be observed that the thermodynamic parameters are increasing with temperature except Gibb's free energy, due to the fact that the vibrational intensities of molecule increase with temperature [71]. The following equations are used to predict approximately the values of heat capacity at constant pressure, enthalpy, Gibb's free energy and entropy for other range of temperature. The regression coefficient is also given in the parabolic equation.

$$C^0_{p,m} = 3.114 + 0.148T - 6.0\times10^{-5}T^2 \qquad (R^2 = 0.9994)$$

$$H^0_m = 2.705 + 0.067T + 4.0\times10^{-5}T^2 \qquad (R^2 = 0.9998)$$

$$G^0_m = -52.493 - 0.096T + 2.0\times10^{-5}T^2 \qquad (R^2 = 0.9994)$$

$$S^0_m = 55.198 + 0.163T - 1.0\times10^{-5}T^2 \qquad (R^2 = 1.0000)$$

Table 11 Thermodynamic properties at different temperatures by B3PW91/6-311+G(d,p) level for N-phenylethanolamine molecule

T (K)	$C^0_{p,m}$ (cal mol^{-1} K^{-1})	ΔH^0_m (kcal mol^{-1})	G^0_m (kcal mol^{-1})	S^0_m (kcal mol^{-1})
100	18.3374	10.5519	−60.9675	71.5194
200	29.3516	17.0891	−71.5106	88.5998
300	41.3258	25.3919	−79.9859	105.3778
400	52.9870	34.8332	−87.6733	122.5066
500	62.9756	45.1410	−94.9327	140.0738
600	71.1650	56.1596	−101.8700	158.0300
700	77.8829	67.7747	−108.5200	176.2950
800	83.4608	79.8926	−114.8990	194.7915
900	88.1431	92.4350	−121.0200	213.4547
1000	92.1040	105.3372	−126.8960	232.2334

CONCLUSION

Based on the density functional theory calculations a complete vibrational analysis has been done by FT-IR and FT-Raman spectroscopic techniques. The vibrational frequencies analysis by B3PW91/6-311+G(d,p) method agrees

satisfactorily with experimental results, compared to LSDA/6-311+G(d,p) method. The geometry optimization exposes the planarity of N-phenylethanolamine molecule. The first hyperpolarizability of NPEA is 5.3 times greater than the value of urea. The Mulliken charge analysis explains the possibilities of charge transfer within the molecule.

The pronounced decrease of the lone pair orbital occupancy and the molecular stabilization energy show the hyperconjucative interaction from the NBO analysis. The NHO represents, the bending angles of different bonds are expressed as the angle of deviation from the direction of the line joining the nuclei centers. The scaled frequencies of the FT-IR and Raman spectra are well consistent with that of the experimental spectra. The strengthening and polarization band increase in IR due to the degree of conjugation, and the O–H bending character reveals the intermolecular hydrogen bonding interactions. Charge transfer occurring in the molecule between HOMO and LUMO energies, frontier energy gap are calculated and presented. The MEP gives the visual representation of the chemically active sites and comparative reactivity of atoms. The thermodynamic functions (heat capacity, enthalpy, Gibb's energy and entropy) from spectroscopic data by statistical methods were obtained for the range of temperature 100–1000 K.

Acknowledgments
One of the author Dr. V. Karunakaran, Assistant Professor, Department of Physics, Government Arts College, Ariyalur – 621 713, Tamil Nadu, is thankful to University Grants Commission (No.F MRP-5131/14 (SERO/UGC/JUNE 2014) for providing fund to this research work.

REFERENCES

[1] J Axelrod, *Pharmacol. Rev.* 18 **1966** 95–113.
[2] E E Inwang, A D Mosnaim, H C Sabelli, *J Neurochem.* 20 **1973** 1469–1473.
[3] H E Shannon, C M Degregorio, *J Pharmacol Exp. Ther*. 222 **1982** 52– 60.
[4] W H Hartung, *Ind Eng Chem* 37 **1945** 126–136.
[5] The Merck Index, 10th Ed., Merck & Co., Rahway. **1983** p. 1051
[6] J Axelrod, J Biol. Chem. 237 **1962** 1657–1660.
[7] M J Frisch, G W Trucks, H B Schlegel et al, Gaussian 2009, Revision A.02 Gaussian, Inc., Wallingford CT, **2009**.
[8] (a) T Sundius, *J. Mol. Struct*. 218 (**1990**) 321.
(b) MOLVIB: A Program for Harmonic Force Field Calculations, QCPE Program No. 604 (**1991**)
[9] T Sundius, *J. Vib. Spectrosc*. **200**2 29 89−95.
[10] A Frisch, A.B. Neilson, A.J. Holder, GAUSSVIEW user Manual, Gaussian Inc., Pittsburgh,CT, **2009**.
[11] PL Polavarapu, *J. Phys. Chem.* **1990** 94 8106−8112.
[12] G Keresztury, S Holly, J Varga, GA Besenyei, Y Wang, JR Durig, *Spectrochim. Acta.* **1993** 49 2007−2017.
[13] JM Chalmers, PR Griffiths, Hand Book of Vibrational Spectroscopy, John Wiley & Sons Ltd, Chichester, **2002**.
[14] A Choperena, P Painter, *Vib. Spectrosc*. **2009** 51 110–118.
[15] M Silverstein, G Clayton Bassler, C Morril, Spectroscopic Identification of Organic Compounds, John Wiley, New York, **1981**.
[16] D N Sathyanarayana, Vibrational Spectroscopy: Theory and Applications, New Age International Publishers, New Delhi, **2007**.
[17] D Michalska, D C Bienko, A J A Bienko, Z Latajaka, *J. Phys. Chem*. **1996** 100 1186–1193.
[18] S George, Infrared and Raman Characteristic Group Frequencies – Tables and Charts, third ed., Wiley New York, **2001**.
[19] R A Nyquist, *Spectrochim. Acta* **1963** 19 1655.
[20] Y Wang, S Saebo, C U Pittman, *J. Mol. Struct*. **1993** 281 91–288.
[21] N Puviarasan, V Arjunan, S Mohan, *Turkey J. Chem*. **2002** 26 323–334.
[22] A Altun, K Golcuk, M Kumru, *J. Mol. Struct. (Theochem.)* **2003** 637 155–169.
[23] V Krishnakumar, R Ramasamy, *Spectrochim. Acta, Part A* **2005** 62 570– 577.
[24] D Lin-Vien, N B Colthup, W G Fateley, J G Grasselli, The Handbook of Infrared and Raman Characteristic Frequencies of Organic Molecules, Academic Press, Boston, MA, **1991**.
[25] L J Bellamy, The Infrared Spectra of Complex Molecules, 3rd ed., John Wiley and Sons Ltd, New York, **1975**.
[26] S Mohan, R Murugan, *Indian J. Pure Appl. Phys*. **1993** 31 496–499.
[27] S Gunasekaran, R Arun Balaji, S Seshadri, S Muthu, *Indian J. Pure Appl. Phys*. **2008** 46 162–168.
[28] R Shanmugam, D Sathyanarayana, *Spectrochim. Acta* **1984** 40 757– 761.
[29] G Varsanyi, Assignments of Vibrational Spectra of Seven Hundred Benzene Derivatives, Vols. 1 and 2, Adam Higler, England, **1974**.
[30] M Snehalatha, C Ravikumar, I Hubert Joe, V S Jayakumar, *J. Raman Spectrosc*. **2009** 40 1121–1126.

[31] K Furic, V Mohack, M Bonifacic, *J. Mol. Struct*. **1992** 267 39–44.
[32] E I Paulraj, S Muthu, *Spectrochim. Acta A* **2013** 106 310–320.
[33] S Sebastian, N Sundaraganesan, *Spectrochim. Acta* **2010** 75 941−952.
[34] G Socrates, Infrared and Raman Characteristic Frequencies, 3rd ed., John Wiley & Sons Ltd., Chichester, **2001**.
[35] D Michalska, *Spectrochim. Acta Part A* **1993** 49 303–307.
[36] P N Prasad, D J Williams, Introduction to Nonlinear Optical Effects in Molecules and Polymers, Wiley, New York, **1991**.
[37] F Meyers, S R Marder, B M Pierce, J L Bredas, *J. Am. Ceram. Soc*. **1994** 116 10703–10703.
[38] C R Zhang, H S Chem, G H Wang, *Chem. Res. Chin. Uni.* **2004** 20 640– 646.
[39] P S Kumar, K Vasudevan, A Prakasam, M Geetha, P M Anbarasan, *Spectrochim. Acta* **2010** 77 45–50.
[40] A D Buckingham, *Adv. Chem. Phys.* **1967** 12 107–142.
[41] O Christiansen, J Gauss, J F Stanton, *Chem. Phys. Lett.* **1999** 305 147– 155.
[42] N Bloembergen, Nonlinear Optics, Benjamin, New York, **1965**.
[43] N F Lane, *Rev. Mod. Phys*. **1980** 52 29.
[44] G Birnbaum (Ed.), Phenomena Induced by Intermolecular Interactions, Plenum, New York, 1980.
[45] G Maroulis, *J. Chem. Phys*. **2000** 113 1813.
[46] D Avci, *Spectrochim. Acta* **2011** 82 37–43.
[47] D Avci, A Basoglu, Y Atalay, *Struct. Chem*. **2010** 21 213–219.
[48] D Avci, H Comert, Y Atalay, *J. Mol. Mod*. **2008** 14 161.
[49] D Avci, *Spectrochim. Acta* **2010** 77 665.
[50] Y X Sun, Q L Hao, W X Wei, Z X Yu, LD Lu, X Wang, Y S Wang, *J. Mol. Struct. Theochem*. **2009** 904 74–82.
[51] J P Foster, F Weinhold, *J. Am. Chem. Soc.* **1980** 102 7211–7218.
[52] A E Reed, L A Curtis, F A Weinhold, *Chem. Rev.* **1988** 88 899–926.
[53] E D Glendening, J K Badenhoop, A E Reed, J E Carpenter, F Weinhold, NBO. Version 3.1, Theoretical Chemistry Institute, University of Wisconsin, Madison, **1996**.
[54] A E Reed, F Weinhold, *J. Chem. Phys*. **1983** 78 4066; A E Reed, F Weinhold, *J. Chem. Phys*. **1985** 83 735–746.
[55] F Weinhold, Natural bond orbital methods, in: P V R Schleyer, N L Allinger, T Clark, J Gasteiger, P A Kollman, H F Schaefer III, PR Schreiner (Eds.), Encyclopedia of Computational Chemistry, vol. 3, John Wiley & Sons, Chichester, **1998**. p. 1792.
[56] F Weinhold, C R Landis, Valency and Bonding: A Natural Bond Orbital Donor–Acceptor Perspective, Cambridge University Press, Cambridge, **2005**.
[57] J Chocholousova, V Vladimir Spirko, P Hobza, *Phys. Chem. Chem. Phys.* **2004** 6 37.
[58] B Smith, Infrared Spectral Interpretation, a Systematic Approach, CRC Press, Washington, DC, 1999.
[59] Y Atalay, D Avci, A Basoglu, *Struct. Chem.* **2008** 19 239 −246.
[60] T Vijayakumar, H Joe, C P R Nair, V S Jayakumar, *Chem. Phys.* **2008** 343 83−99.
[61] L J Na, C Z Rang, Y S Fang, J Zhejiang *Univ, Science* **2005** *6* 584–589.
[62] PK Chattraj, B Maiti, U J Sarkar, *J. Phys. Chem.* **2003** 107 4973–4975.
[63] R G Parr, R A Donnelly, M Levy, W E Palke, *J. Am. Chem. Soc*. **1978** 68 3801–3807.
[64] R G Parr, R G Pearson, *J. Am. Chem. Soc.* **1983** 105 7512–7516.
[65] R G Parr, P K Chattraj, *J. Am. Chem. Soc*. **1991** 113 1854–1855.
[66] R P Iczkowski, J V Margrave, *J. Am. Chem. Soc*. **1961** 83 3547–3551.
[67] L Larabi, Y Harek, O Benali, S Ghalam, *Prog. Org. Coat.* **2005** 54 256–262.
[68] R G Parr, L V Szentpaly, S Liu, *J. Am. Chem. Soc.* **1999** 121 1922−1924.
[69] E Scrocco, J Tomasi, *Adv. Quantum Chem*. **1978** 11 115–121.
[70] R S Mulliken, *J Chem. Phys*. **1955** 23 1833–1840.
[71] J Bevan Ott, J Boerio-goates, Calculations from Statistical Thermodynamics, Academic Press, **2000**.